2. N. G. Hairston, F. E. Smith, L. B. Slobodkin, *Am. Nat.* **94**, 421 (1960).
3. S. L. Pimm, *The Balance of Nature* (Univ. of Chicago Press, Chicago, IL, 1992), chap. 14.
4. We considered the model in G. Caughley, *Analysis of Vertebrate Populations* (Wiley, New York, 1977), pp. 130–132.
5. A. T. Bergerud, *Trends Ecol. Evol.* **3**, 68 (1988); *Can. J. Zool.* **64**, 1515 (1986).
6. R. O. Peterson, R. E. Page, K. M. Dodge, *Science* **224**, 1350 (1984).
7. R. O. Peterson and R. E. Page, *J. Mammal.* **69**, 89 (1988); *Acta Zool. Fenn.* **174**, 251 (1983).
8. K. L. Risenhoover, thesis, Michigan Technological University (1987), p. 49.
9. R. A. Janke, D. McKaig, R. Raymond, *For. Sci.* **24**, 115 (1978); B. E. McLaren, unpublished data (figures are for the west end of Isle Royale).
10. J. D. Snyder and R. A. Janke, *Am. Midl. Nat.* **95**, 79 (1976).
11. Suppression of balsam fir growth on Isle Royale by moose foraging occurs because of continuous removal of upper branches in winter. Trees remain alive in the forest understory for several decades, because lateral branches are protected from browsing by snow cover and because balsam fir is tolerant of shade. Trees in this study (except those represented in Fig. 4A) ranged from 34 to 68 years of age but came from a consistent height interval of 1 to 3 m at the time of sampling. The age variation made no contribution to variation in growth rates.
12. T. A. Brandner, R. O. Peterson, K. L. Risenhoover, *Ecology* **71**, 155 (1991).
13. G. Caughley and A. Gunn, *Oikos* **67**, 47 (1993); S. L. Pimm and A. Redfearn, *Nature* **334**, 613 (1984); M. H. Williamson, *The Analysis of Biological Populations* (Arnold, London, 1982), chap. 5.
14. A harmonic function fitted with an ordinary least squares approach, period 17.8 years, matched the west-end chronology with $R^2 = 0.38$; a function with period 16.1 years matched the east-end chronology with $R^2 = 0.70$. Following M. G. Bulmer [*J. Anim. Ecol.* **43**, 701 (1978)], functions incorporating both a harmonic term and a first-order autoregressive term were matched to the series, with improved fits of $R^2 = 0.68$ and $R^2 = 0.81$, respectively.
15. The cycle period inferred from empirical consideration of the three-trophic-level system is shorter than a period cited earlier, which was derived from a body-mass regression (*6*). However, the confidence interval for the allometric equation also included the shorter period of 16 to 18 years.
16. Ring-width suppression followed height-growth suppression in both samples by about 3 years.
17. G. Caughley, *Oecologia* **54**, 309 (1976). The plant with the inferior growth rate lags behind herbivore density more than does the plant with the superior growth rate.
18. B. E. McLaren, unpublished data; R. M. Linn, thesis, Duke University (1957).
19. R. O. Peterson, unpublished data.
20. Our result is new primarily because studies of long-term processes in terrestrial food chains are rare, especially studies of those in which top carnivores still exist. A. R. E. Sinclair and colleagues [*Am. Nat.* **141**, 173 (1993)] recently described the well-known snowshoe hare (*Lepus americana*) cycle in the Yukon Territory, Canada, as generating cyclic suppression of white spruce (*Picea glauca*). These authors, however, favored an explanation in meteorological driving forces. Other studies [for example, L. B. Keith, A. W. Todd, C. J. Brand, R. S. Adamcik, D. H. Rusch, *Int. Congr. Game Biol.* **13**, 151 (1976); L. B. Keith and L. A. Windberg, *Wildl. Monogr.* **58**, 70 (1978)] have considered plant-herbivore and herbivore-carnivore relations for the snowshoe hare, but in different study areas. The third trophic level in the fox-prey system studied by E. R. Lindström and colleagues [*Ecology* **75**, 1042 (1994)] was a parasite.
21. J. M. Thurber and R. O. Peterson, *J. Mammal.* **74**, 879 (1993).
22. D. J. McQueen, M. R. S. Johannes, J. R. Post, T. J. Stewart, D. R. S. Lean, *Ecol. Monogr.* **59**, 289 (1989); S. R. Carpenter *et al.*, *Ecology* **68**, 1863 (1987); M. Lynch and J. Shapiro, *Limnol. Oceanogr.* **26**, 86 (1981); J. L. Brooks and S. I. Dodson, *Science* **150**, 28 (1965).
23. L. Oksanen, S. D. Fretwell, J. Arruda, P. Niemela, *Am. Nat.* **118**, 240 (1981); for other contrasting published ideas concerning predator-prey cycles on Isle Royale, see (*6*) and J. Pastor and R. J. Naiman, *Am. Nat.* **139**, 690 (1992).
24. M. L. Rosenzweig, *Am. Nat.* **102**, 67 (1968). The index was calculated with the use of daily records from Thunder Bay, Ontario.
25. Understory fir density exceeds 250 ha^{-1} over about 70% of Isle Royale's land area and exceeds 10,000 ha^{-1} in many shoreline forests. Values were obtained by averaging density estimates for stems ≤2 m in 0.01-ha plots at the corners of each (square-mile) township section.
26. The ring-width index is the ratio of increments calculated as a summation of volume differences for a series of stacked conic sections representing the stems of sampled trees, divided by the cambial surface area at the beginning of each growing season for each year. An aggregate index, comprising ring-width measurements ($\pm 10^{-2}$ mm) averaged for four radii at 5- to 10-cm increments along stems, is presented. This intensity of sampling permits an accurate height-growth reconstruction of the trees and measurement of the wood volume increment throughout the trees' stems.
27. We acknowledge the National Park Service (NPS) for permission to sample trees; V. G. Smith, University of Toronto, for the design of the ring-width index; R. J. Miller, Ontario Ministry of Natural Resources, for the development of analytic software and loan of measurement equipment; Environment Canada for supplying weather records; and the following for financial support: National Geographic Society, NPS Earthwatch, the Boone and Crockett Club, and NSF grant DEB-9317401. W. C. Kerfoot and F. H. Wagner kindly reviewed this manuscript and offered many helpful suggestions.

13 May 1994; accepted 6 September 1994

Requirement for Intron-Encoded U22 Small Nucleolar RNA in 18*S* Ribosomal RNA Maturation

Kazimierz T. Tycowski, Mei-Di Shu, Joan A. Steitz*

The nucleoli of vertebrate cells contain a number of small RNAs that are generated by the processing of intron fragments of protein-coding gene transcripts. The host gene (*UHG*) for intron-encoded human U22 is unusual in that it specifies a polyadenylated but apparently noncoding RNA. Depletion of U22 from *Xenopus* oocytes by oligonucleotide-directed ribonuclease H targeting prevented the processing of 18S ribosomal RNA (rRNA) at both ends. The appearance of 18S rRNA was restored by injection of in vitro–synthesized U22 RNA. These results identify a cellular function for an intron-encoded small RNA.

The nucleolus is the site of rRNA synthesis, processing, and assembly into ribosomes (*1*). In vertebrate cells, rRNA is transcribed as a 40 to 47S precursor that is subsequently cleaved at multiple sites to yield the mature 18S, 28S, and 5.8S rRNAs. The nucleolus also contains small nucleolar ribonucleoproteins (snoRNPs), each composed of a short RNA, known as snoRNA, and at least one protein (*2*). On the basis of their mode of synthesis, vertebrate snoRNAs of the U series fall into two classes. U3, U8, and U13 RNAs are transcribed as independent units by RNA polymerase II and carry 5′-trimethylguanosine caps (*3*). In contrast, snoRNAs U14 through U21 are all encoded within introns of genes for abundantly expressed proteins. They mature by intron processing mechanisms, as yet poorly defined, and possess monophosphates at their 5′ ends (*2*). Most snoRNAs are associated with a conserved nucleolar antigen, fibrillarin (*2*, *3*).

Several snoRNPs have been shown to function in rRNA processing (*2*). The most abundant, U3, is essential for cleavage within the 5′ external transcribed spacer (ETS) of both vertebrate (*4*, *5*) and yeast (*6*) precursor rRNAs (pre-rRNAs) and may contribute to 18S and 5.8S rRNA formation as well (*6*, *7*). Yeast U14, which is not intron-encoded, and snR30 (small nuclear RNA 30) are required for cell viability and accumulation of 18S rRNA (*8*), whereas yeast ribonuclease (RNase) MRP is essential for 5.8S rRNA maturation (*9*) and snR10 enhances growth and processing of the 35S pre-rRNA (*10*). *Xenopus* U8 is the only snoRNA found to function in vertebrate 28S and 5.8S rRNA processing (*11*).

Human RNA Y (*3*), now renamed U22, is a fibrillarin-associated snoRNA that contains a 5′-monophosphate and has the potential to form a terminal stem-loop-stem motif with conserved boxes C and D (*12*). We completed sequence analysis of human U22 RNA and also determined the nucleotide sequence of two (A and B) *Xenopus* U22 genes that differ only at positions 28 and 41 (Fig. 1A). Human and *Xenopus* U22 RNAs are ~75% identical, with the identities confined mostly to the termini and a middle section of the molecule. Neither shows significant homology to other known RNAs.

Southern (DNA) blot analysis of genomic DNA detected a single locus for human U22 (*13*), another feature that distinguishes

Howard Hughes Medical Institute, Department of Molecular Biophysics and Biochemistry, Yale University School of Medicine, 295 Congress Avenue, New Haven, CT 06536, USA.

*To whom correspondence should be addressed.

intron-encoded snoRNAs from independently transcribed small nuclear RNAs, which usually arise from multiple genes (*14*). To investigate the U22 host gene (*UHG*), we isolated a Charon 4A clone containing a human genomic DNA fragment (*15*) that was more than 10 kb long; sequence analysis of 2 kb of this clone revealed a 125-nucleotide (nt) region colinear with U22 RNA (Fig. 1B). A potential polyadenylation signal, composed of an AATAAA hexamer followed by a CA cleavage site and GT-rich sequences, was found ~0.9 kb downstream from the U22-coding region. Two λgt11 clones, *UHG.3* and *UHG.8*, whose 1.36- and 1.1-kb complementary DNA (cDNA) inserts both possess polyadenylate tails at their 3′ ends, were isolated and sequenced (Fig. 1C) (*15*).

Comparison of the genomic sequence with that of the cDNA clones revealed that the U22 RNA gene is located within the penultimate intron of an uncharacterized human gene that specifies a polyadenylated RNA (Fig. 1B). Northern (RNA) blot analysis of HeLa cell polyadenylated RNA with the *UHG.3* cDNA probe revealed a single RNA species of ~1400 nt whose abundance was comparable to that of γ-actin mRNA (*13*). The agreement in size between this cellular RNA and the *UHG.3* cDNA indicated that a nearly full-length cDNA had been isolated.

Unexpectedly, the longest open reading frame (ORF), at nucleotides 239 to 433 of the *UHG.3* cDNA, encoded only 65 amino acids (Fig. 1C). If this 65–amino acid polypeptide is a product of the *UHG* gene in vivo, the *UHG* mRNA would be unusual in three respects. (i) Its 5′ untranslated region (UTR) would contain at least six AUGs. AUG codons in 5′ UTRs block translation from downstream ORFs and require special regulatory mechanisms to overcome inhibition (*16*). (ii) The coding sequence for the 3′ UTR would be interrupted by at least five introns, a situation unprecedented in vertebrates (*17*). (iii) The putative initiator AUG for the 65–amino acid ORF would lie within an unfavorable context for translation initiation (GACCUAAUGU versus the GCCPuCCAUGG consensus, where Pu is purine) (*16*). We therefore speculate that *UHG* RNA, although polyadenylated, does not serve as a mRNA but is instead the final product of the *UHG* gene.

Several apparently noncoding polyadenylated RNAs have been previously identified. Vertebrate *H19* and *Xist* RNAs, as well as *Drosophila* hsr-omega-n and hsr-omega-c RNAs, have each been suggested to perform regulatory functions in the cell (*18*). Unlike these RNAs, whose expression is either tissue-, developmental stage–, or sex-specific, *UHG* RNA is presumably expressed in all cells to ensure the production of U22 RNA. We cannot rule out the possibility that a longer ORF in *UHG* RNA is generated either by frameshift translation or by RNA editing (*19*).

To investigate whether U22 RNA functions in rRNA processing, we targeted this RNA for destruction by injecting antisense deoxyoligonucleotides into *Xenopus* oocytes (*11*, *20*). A single injection into the cytoplasm of an oligonucleotide complementary to either positions 37 to 53 or 53 to 67 of U22 RNA (Fig. 2A, lanes 2 and 3), but not of a control oligonucleotide (lane 4), caused efficient degradation of U22 RNA as assayed by primer extension. The amount of another snoRNA, U15, remained unchanged. Six hours later, we injected [α-^{32}P]uridine triphosphate (UTP) into U22-depleted oocytes, incubated them overnight, and then manually dissected them into germinal vesicles (GVs) and cytoplasms. Total RNAs from each compartment were analyzed on agarose and polyacrylamide gels (Fig. 2, B and C). The cytoplasm accumulates labeled mature rRNAs that are synthesized and exported from the nucleus over the course of the labeling, whereas the GV contains mature 18S and 28S rRNAs that have not yet been exported plus rRNA precursors. In contrast to control oocytes, oocytes injected with U22(37–53) or U22(53–67) oligonucleotide contained no labeled 18S rRNA (Fig. 2B). Instead, the 20S precursor to 18S rRNA accumulated in the nucleus. Because *Xenopus* 20S possesses spacer regions at both ends (Fig. 2D) (*7*), we conclude that U22 depletion prevents cleavage events at both the 5′ and 3′ termini of 18S rRNA. Inhibition of cleavage at the 3′ end of 18S also resulted in the disappearance of the 36S precursor to 28S and 5.8S rRNA, as expected.

Normal rRNA processing in U22-depleted oocytes was restored by subsequent injection of in vitro–transcribed U22 RNA (Fig. 3, lanes 3 and 8), but not by the vector polylinker (lanes 4 and 9) or antisense U22 transcripts (lanes 5 and 10). The "rescue transcript," which contained 26 and 20 nt at the 5′ and 3′ ends, respectively, of U22-

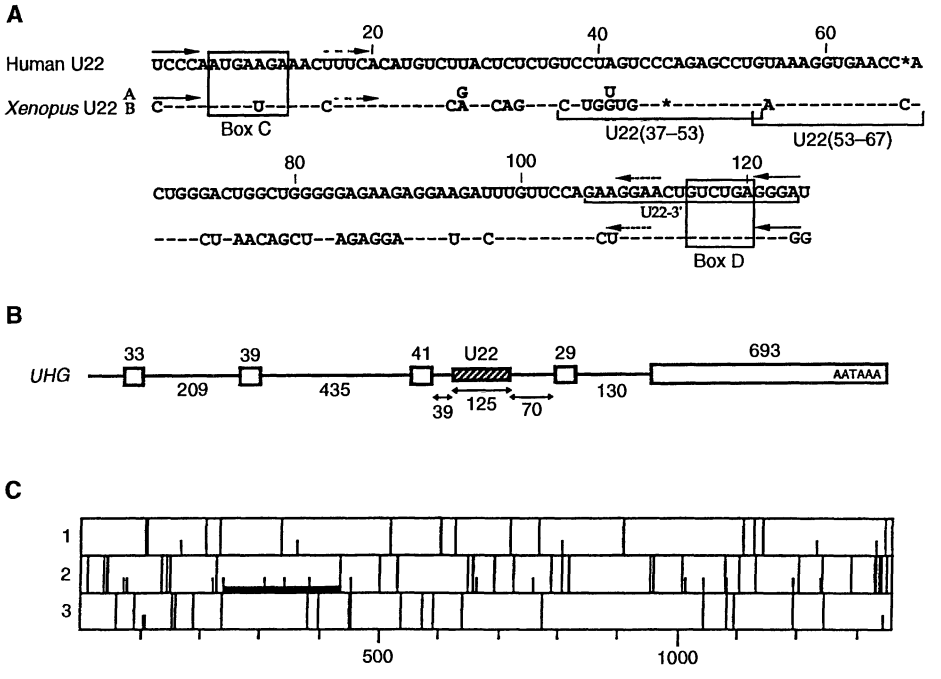

Fig. 1. (**A**) Comparison of the human and *Xenopus* U22 snoRNA sequences. For the enzymatic sequencing of the last 35 nucleotides of human U22, HeLa cell RNAs were immunoprecipitated with the 72B9 monoclonal antibody to fibrillarin and labeled on the 3′ end as described (*3*). After fractionation on 8% denaturing polyacrylamide gels, U22 RNA was sequenced as described (*12*). About 90 5′ nucleotides of human or partial sequences of *Xenopus* U22 RNAs were determined by primer extension (*27*) with the use of the U22-3′ primer and total HeLa or *Xenopus* epithelial tissue culture (XTC) cell RNA as a template, respectively. By inverted or standard PCR amplification (*28*), respectively, we cloned and sequenced flanking or coding regions of two (A and B) *Xenopus* U22 RNA genes. Identical or missing nucleotides are represented by dashes or asterisks, respectively. Solid and dashed arrows indicate complementary nucleotides that form two stems. Conserved boxes C and D as well as regions complementary to U22(37–53), U22(53–67), and U22-3′ deoxyoligonucleotides are marked. (**B**) Schematic representation of the 3′ portion of the human U22 host gene. (**C**) ORFs in three reading frames in *UHG.3* cDNA. Short and long vertical bars within each frame indicate possible translation start and stop codons, respectively. The longest (65–amino acid) ORF is designated by a horizontal bar. Nucleotides are numbered below. The *UHG.8* cDNA begins at nucleotide 267. The GenBank accession numbers for *Xenopus* U22 RNA and human *UHG* genomic DNA and *UHG.3* cDNA are L36586, L36588, and L36587, respectively.

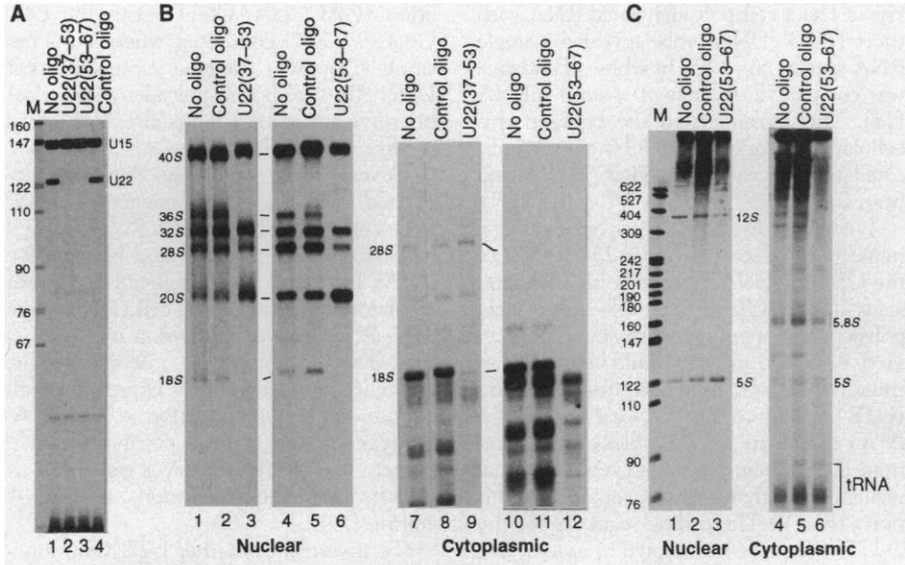

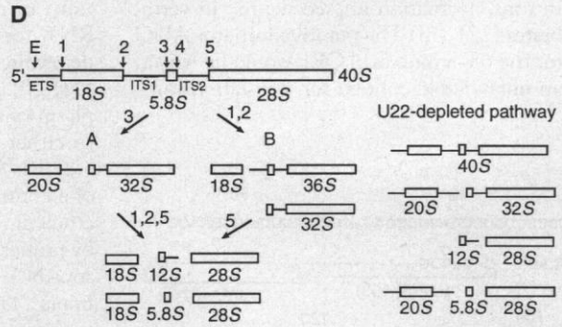

Fig. 2. Ribosomal RNA processing in U22-depleted oocytes. Oocytes were cytoplasmically injected with U22(37–53), U22(53–67), or a control deoxyoligonucleotide (5′-ATCTGGAATCTACCTGCC-3′) (*29*). Six hours later, the oocytes were injected with [α-^{32}P]UTP; after an 18-hour incubation, they were dissected and RNA was isolated from both nuclear and cytoplasmic compartments (*29*). In (**A**), the RNA was probed for U15 and U22 snoRNAs by primer extension (*27*) with the use of a mixture of U15-3′ (5′-CTTCTCAGACAAATG CC-3′) and X-U22-3′ (5′-CCCTCAGACAGTTCCAG-3′) primers. In (**B**), RNAs were resolved on horizontal 1% agarose-formaldehyde gels and transferred to Zeta-Probe membranes (Bio-Rad) (*26*). Membranes were baked at 80°C for 1 hour and subjected to autoradiography. In (**C**), RNAs were separated on 8% denaturing polyacrylamide gels, which were dried and subjected to autoradiography directly. In (A) and (C), lane M contains DNA size markers. Note that oocytes injected with U22-specific oligonucleotides also produce less 28*S* [(B), lanes 3 and 6] and 12*S* [(C), lane 3] rRNA. The decrease in 28*S* rRNA is usually apparent in the cytoplasm [Fig. 3, lanes 7, 9, and 10 (*13*)]. (**D**) Alternative pathways for rRNA processing in *Xenopus* oocytes. The 40*S* precursor includes 5′ ETS (712 nt), 18*S* rRNA (1825 nt), ITS1 (557 nt), 5.8*S* rRNA (162 nt), ITS2 (262 nt), and 28*S* rRNA (4110 nt). In pathways A and B, the cleavages occur in a different temporal order. Shown are the long-lived precursors and the mature rRNAs. Also shown is the pathway in oocytes depleted of U22 snoRNA. Arrows indicate processing sites that occur at or in the proximity of the termini of the mature rRNAs; E stands for the early processing site.

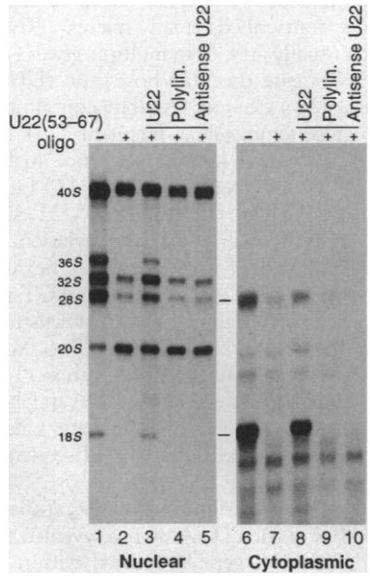

Fig. 3. Rescue of rRNA processing defects in U22-depleted oocytes by in vitro–transcribed U22 RNA. Oocytes were cytoplasmically injected with U22(53–67) oligonucleotide (lanes 2 to 5 and 7 to 10) (*29*); then U22 (lanes 3 and 8), polylinker (lanes 4 and 9), or antisense U22 (lanes 5 and 10) transcripts were injected into germinal vesicles (*29*). After overnight labeling, RNAs from both nuclear and cytoplasmic compartments (*29*) were resolved on horizontal 1% agarose-formaldehyde gels and transferred to Zeta-Probe membranes (Bio-Rad) (*26*). Membranes were baked at 80°C for 1 hour and subjected to autoradiography. Note that production of 28*S* (lanes 3 and 8) and 12*S* (*13*) rRNAs was also increased by the U22 rescue transcript.

flanking sequences as well as short vector-related sequences, was processed in oocytes to U22 RNA (*13*). This rescue experiment confirms that the 18*S* processing defect can be ascribed specifically to U22 depletion.

With the use of Northern blot analyses of nuclear RNAs, we established that the 20*S* RNA that accumulates in U22-depleted oocytes contains the same termini as the normal 20*S* precursor to 18*S*. The probes were an oligonucleotide complementary to positions 31 to 48 of the 5′ ETS and three oligonucleotides, ITS1-3A, ITS1-3B, and ITS1-4, complementary to the 3′ portion of the internal transcribed spacer 1 (ITS1) at positions 421 to 436, 492 to 510, and 521 to 557, respectively. The last probe directly abuts the 5′ end of 5.8*S* rRNA. The ETS probe hybridized to both 40*S* and 20*S* pre-rRNAs from normal as well as U22-depleted oocytes (Fig. 4A), which is consistent with the finding (*5*) that early processing at residue 105 of the 5′ ETS is very inefficient in *Xenopus* oocytes. The ITS1-3A probe hybridized to 20*S* RNA in both normal and U22-depleted oocytes (Fig. 4B, left panel), whereas neither ITS1-3B nor ITS1-4 did. We conclude that both 20*S* RNAs contain the entire 5′ ETS, 18*S* RNA, and ITS1 lacking only the last ~100 nt. These results refine the earlier 3′ end assignment for *Xenopus* 20*S* (*11*).

The last ~100 nt of ITS1 are also missing from the normal 32*S* pre-rRNA because the ITS1-3B and ITS1-4 probes likewise failed to hybridize to this precursor in control oocytes. Their weak but reproducible hybridization to 32*S* RNA in U22-depleted oocytes [Fig. 4B, lanes 7, 10 and 11 (*13*)] suggests that the 5′ end of 5.8*S* rRNA is created by an initial cleavage within ITS1 (between probes ITS1-3A and ITS1-3B) followed by rapid exonucleolytic trimming, which is slowed by U22 depletion. This is reminiscent of the situation in yeast, where processing at site A3, which requires RNase MRP, is followed by rapid 5′ to 3′ exonucleolytic activity to generate the 5′ end of 5.8*S* rRNA (*9*). In mouse, cleavage at site 3 was deduced to occur either directly at or only 6 to 7 nt upstream of the 5′ end of 5.8*S* rRNA (*21*); but in rat, the 5′ ends of 32*S* and 12*S* pre-rRNAs have been mapped ~160 nt upstream of 5.8*S* rRNA (*22*).

A distinguishing feature of 18*S* rRNA processing in *Xenopus* oocytes is that cleavage at site 1 occurs later than it does in other vertebrates (*1*). As a result, oocyte 20*S* RNA retains the 5′ ETS, which is not present on the 20*S* precursors to 18*S* rRNA from other species; and 38*S* pre-rRNA, a direct product of cleavage of the 40*S* precursor at site 1, is not visible in oocytes after overnight labeling of the RNA (*7*, *11*). The lack of accumulation in U22-depleted oocytes of either

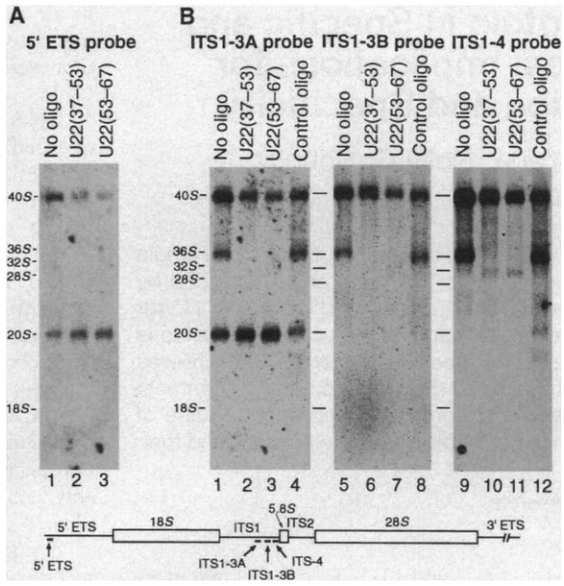

Fig. 4. Mapping the ends of the 20*S* precursor. Sixteen hours after injection with the indicated deoxyoligonucleotides, oocytes were dissected and nuclear RNA was isolated (*29*). RNAs were resolved on 1% agarose-formaldehyde gels and transferred to Zeta-Probe membranes (*26*). The membranes were baked for 1 hour at 70°C and hybridized with the 5′ ETS (**A**) or one of the ITS1 (**B**) probes (*30*) as indicated. Hybridizations with the 5′ ETS, ITS1-3A, and ITS1-3B probes were carried out in 1 M NaCl, 10% dextran sulfate, 1% SDS, and sonicated salmon sperm DNA (200 μg/ml) at 37°C. Hybridizations with the ITS1-4 probe were carried out in 6× saline sodium citrate (SSC), 50% formamide, 0.5% SDS, 5× Denhardt's solution, and sonicated salmon sperm DNA (100 μg/ml) at 37°C. For hybridization, 2 × 10^6 cpm (specific activity, 2 Ci/μmol) of the probes was used. The final washings were in 1× SSC and 0.5% SDS at 50°C.

38*S* or other intermediates processed at only one end of 18*S* argues further that cleavages at the termini of oocyte 18*S* rRNA are coordinated. Alternatively, cleavage at site 1 in oocytes could normally be rapidly followed by a cut at site 2, with both cuts being independently prevented by U22 depletion. Detection of a 38*S* precursor cleaved only at site 1 in *Xenopus* somatic cells (*23*) lends support to the latter explanation. The recent identification in HeLa cells of a 30*S* pre-rRNA (*24*) that seems to correspond to the *Xenopus* 20*S* precursor implies that the predominant pathway for 18*S* maturation in the *Xenopus* oocyte also exists in other vertebrates, although it is used less efficiently.

In yeast, a similar phenotype to that observed upon depletion of *Xenopus* U22—accumulation of a longer precursor to 18*S* that contains spacer sequences at both ends—has been reported after genetic depletion of U3, U14, snR10, or snR30 snoRNA, as well as of several protein factors (*6*, *8*, *10*, *25*). These components have therefore been suggested to assemble into a multi-snoRNP complex required for the maturation of 18*S* rRNA in eukaryotes. Vertebrate intron-encoded U22 snoRNA represents another addition to this growing list.

REFERENCES AND NOTES

1. A. A. Hadjiolov, *The Nucleolus and Ribosome Biogenesis* (Springer-Verlag, New York, 1985); B. Sollner-Webb, K. T. Tycowski, J. A. Steitz, in *Ribosomal RNA: Structure, Evolution, Gene Expression and Function in Protein Synthesis*, A. E. Dahlberg and R. A. Zimmermann, Eds. (CRC Press, Boca Raton, FL, in press).
2. M. J. Fournier and E. S. Maxwell, *Trends Biochem. Sci.* **19**, 131 (1993); B. Sollner-Webb, *Cell* **75**, 403 (1993); W. Filipowicz and T. Kiss, *Mol. Biol. Rep.* **18**, 149 (1993).
3. K. Tyc and J. A. Steitz, *EMBO J.* **8**, 3113 (1989).
4. R. L. Maser and J. P. Calvet, *Proc. Natl. Acad. Sci. U.S.A.* **86**, 6523 (1989); I. L. Stroke and A. M. Weiner, *J. Mol. Biol.* **210**, 497 (1989); S. Kass, K. Tyc, J. A. Steitz, B. Sollner-Webb, *Cell* **60**, 897 (1990).
5. E. B. Mougey, L. K. Pape, B. Sollner-Webb, *Mol. Cell. Biol.* **13**, 5990 (1993).
6. J. M. X. Hughes and M. Ares Jr., *EMBO J.* **10**, 4231 (1991); M. Beltrame and D. Tollervey, *ibid.* **11**, 1531 (1992).
7. R. Savino and S. A. Gerbi, *ibid.* **9**, 2299 (1990).
8. H. V. Li, J. Zagorski, M. J. Fournier, *Mol. Cell. Biol.* **10**, 1145 (1990); J. P. Morrissey and D. Tollervey, *ibid.* **13**, 2469 (1993).
9. M. E. Schmitt and D. A. Clayton, *ibid.* **13**, 7935 (1993); S. Chu, R. H. Archer, J. M. Zengel, L. Lindahl, *Proc. Natl. Acad. Sci. U.S.A.* **91**, 659 (1994); Y. Henry *et al.*, *EMBO J.* **13**, 2452 (1994).
10. D. Tollervey and C. Guthrie, *EMBO J.* **4**, 3873 (1985); D. Tollervey, *ibid.* **6**, 4169 (1987).
11. B. A. Peculis and J. A. Steitz, *Cell* **73**, 1233 (1993); *Genes Dev.* **8**, 2241 (1994).
12. K. T. Tycowski, M.-D. Shu, J. A. Steitz, *Genes Dev.* **7**, 1176 (1993).
13. ———, unpublished results.
14. J. A. Dahlberg and E. Lund, in *Structure and Function of Major and Minor Small Nuclear Ribonucleoprotein Particles*, M. L. Birnstiel, Ed. (Springer-Verlag, Berlin, 1988), pp. 38–70.
15. The Charon 4A genomic library was screened with the human U22 DNA probe. For screening the λgt11 placental cDNA library, a *UHG* DNA probe encompassing the polyadenylate signal and extending 0.26 kb upstream was used. Hybridizations were carried out in 5× SSPE (180 mM NaCl, 10 mM Na_2HPO_4, and 1 mM EDTA), 50% formamide, 0.1% SDS, 5× Denhardt's solution (0.1% Ficoll, 0.1% polyvinylpyrrolidone, and 0.1% bovine serum albumin), and sonicated salmon sperm DNA (100 μg/ml) at 42°C, and the final washings were in 0.1× saline sodium citrate and 0.5% SDS at 65°C.
16. M. Kozak, *J. Cell Biol.* **115**, 887 (1991).
17. J. D. Hawkins, *Nucleic Acids Res.* **16**, 9893 (1988).
18. K. Pfeifer and S. M. Tilghman, *Genes Dev.* **8**, 1867 (1994); N. C. Hogan, K. L. Traverse, D. E. Sullivan, M.-L. Pardue, *J. Cell Biol.* **125**, 21 (1994).
19. J. F. Atkins, R. B. Weiss, R. F. Gesteland, *Cell* **62**, 413 (1990); L. M. Powell *et al.*, *ibid.* **50**, 831 (1987).
20. C. Prives and D. Foukal, *Methods Cell Biol.* **36**, 185 (1991).
21. L. H. Bowman, W. E. Goldman, G. I. Goldberg, M. B. Hebert, D. Schlessinger, *Mol. Cell. Biol.* **3**, 1501 (1983).
22. K. V. Hadjiolova, O. I. Georgiev, V. V. Nosikov, A. A. Hadjiolov, *Biochim. Biophys. Acta* **782**, 195 (1984).
23. P. K. Wellauer and I. B. Dawid, *J. Mol. Biol.* **89**, 379 (1974).
24. K. V. Hadjiolova, M. Nicoloso, S. Mazan, A. A. Hadjiolov, J.-P. Bachellerie, *Eur. J. Biochem.* **212**, 211 (1993).
25. D. Tollervey, H. Lehtonen, M. Carmo-Fonseca, E. C. Hurt, *EMBO J.* **10**, 573 (1991); J.-P. Girard *et al.*, *ibid.* **11**, 673 (1992); R. Jensen, D. Tollervey, E. C. Hurt, *ibid.* **12**, 2549 (1993).
26. J. Sambrook, E. F. Fritsch, T. Maniatis, *Molecular Cloning: A Laboratory Manual* (Cold Spring Harbor Laboratory, Cold Spring Harbor, NY, ed. 2, 1989).
27. K. A. Parker and J. A. Steitz, *Mol. Cell. Biol.* **7**, 2899 (1987).
28. For inverted polymerase chain reaction (PCR), total *Xenopus* red blood cell DNA (2 μg) was digested with Msp I, extracted with PCA [phenol:chloroform:isoamyl alcohol (25:25:1)], and ethanol-precipitated, and the DNA was made circular as described (*12*). The DNA was subsequently phenol-extracted, ethanol-precipitated, and used for PCR amplification with primers 5′-ATGTGAAGGTTTCATCATTGG-3′, and 5′-GCGAGAGCCTGAAAAGGTGAAC-3′. For PCR amplification of the U22A or U22B coding regions, 5′-CCAAGTCTGTTGCTAATGACG-3′ and 5′-CTTCATTACAATGAGGTTCATC-3′ or 5′-GTACAATGTGTTCTTGTTAATG-3′ and 5′-CACAAAATCATAAATATAAGCC-3′ primers, respectively, and undigested DNA were used. The amplification reactions were as described (*12*). The PCR products were cloned into the Sma I site of the pGEM3Z vector. DNA sequencing was performed with a Sequenase kit (U.S. Biochemicals) according to the manufacturer's protocol.
29. Thirty nanoliters of U22(37–53), U22(53–67), or control deoxyoligonucleotide at a concentration of 3 mg/ml, 1 mg/ml, or 3 mg/ml, respectively, was injected into the cytoplasm of stage 5 and early stage 6 oocytes. After incubation in modified Barth's saline for the indicated time at 18°C, oocytes were reinjected with 150 nCi of [α-^{32}P]UTP at a concentration of 5 mCi/ml (3000 Ci/mmol) and incubated overnight. For RNA isolation, the oocytes were manually dissected into GVs and cytoplasms in buffer containing 3.25 mM Na_2HPO_4, 1.75 mM KH_2PO_4, 17 mM NaCl, 83 mM KCl, and 10 mM $MgCl_2$, collected into Eppendorf tubes, and stored on dry ice. Each sample receive 20 μl of homogenization buffer [50 mM NaCl, 50 mM tris-HCl (pH 7.5), 5 mM EDTA, 0.5% SDS, and proteinase K (200 μg/ml)] and was incubated at 37°C for 15 min. RNA was extracted twice with PCA and precipitated with ethanol. For "rescue" experiments, GVs were injected with U22 or control RNAs (25 nl, 2.4 nmol/ml) 15 hours after the oligonucleotide injection. Five hours later, [α-^{32}P]UTP was injected into the cytoplasm; oocytes were incubated overnight and dissected, and RNA was isolated as above. The U22 rescue transcript and antisense U22 were prepared by transcription of pGEM3Z.U22 plasmid with T7 and SP6 polymerase, respectively. The pGEM3Z.U22 contained *Xenopus* U22B plus 26 and 20 nt of the 5′ and 3′ flanking sequences, respectively, inserted into the Sma I site. For transcription of sense or antisense U22, the plasmid was linearized with Hind III or Eco RI, respectively. The polylinker transcript was synthesized by T7 polymerase from the pGEM3Z vector cut with Hind III.
30. The 5′ ETS (5′-CGGTCCTTTTTTCGGGCG-3′), ITS1-3A (5′-GGGTCCTGCGGCGGCG-3′), and ITS1-3B (5′-CTACCGGTGCTGCCGCTGA-3′) probes were 5′ end-labeled with [γ-^{32}P]adenosine triphosphate and polynucleotide kinase (*26*). The ITS1-4 probe was prepared by filling in with the Klenow fragment (*12*) the single-stranded regions of DNA formed by oligonucleotides 5′-ACCGAAAAGGAAAACCGACCGACGCG-3′ and 5′-GCTCTCGCCGACGCGTCGGTCGG-3′, whose 3′ terminal 12 nt are complementary to each other.

31. We thank B. Peculis for guidance and advice on oocyte injections and for the ITS1-4 probe; S. Baserga and V. Myer for the λgt11 cDNA library; members of the Steitz laboratory for discussion; and B. Peculis, V. Myer, E. Scharl, and L. Otake for critical reading of the manuscript. Supported by grant GM26154 from the NIH.

12 August 1994; accepted 30 September 1994